GEOLOGICAL CONSTRAINS IN THE CRS PARAMETER SEARCH

S. Dümmong and D. Gajewski

email: *sdu@statoil.com*

keywords: *Multi-parameter stacking; CRS parameters, geological constraints*

ABSTRACT

We briefly review Common Reflection Surface (CRS) stacking and describe its current implementation and parameter determination strategy. Since the CRS stacking operator depends on three stacking parameters in the 2D case, a global simultaneous parameter determination is expensive. Therefore, the parameter search is divided into subsequent 1D searches. One parameter is determined in the CMP domain and the two others in the Zero Offset (ZO) domain. To improve and accelerate the parameter determination, we introduce geological constraints into this procedure. First, we assume that the stacking velocity is smoothly increasing with time. Based on this, we implemented a scheme to dynamically restrict the stacking velocity parameter intervals. The assumption is not fulfilled for every geological situation, but can be applied in many cases. Second, we assume dominant geological dips in the stacked section, which leads to dip filtering in the corresponding data space, i.e., in the ZO sections. The assumption that reflections and unwanted events have different dips, is not always satisfied, but can be applied when a priori geological information of the subsurface is available. Results of the constrained parameter search obtained for field data from the Eastern Mediterranean/Levantine basin indicate the potential of the approach. The constrained parameter search emphasizes reflections, reduces scattered energy and provides improved CRS attributes which is beneficial for all following processing steps in the CRS workflow. The latter is of major importance even if the improvement in the stacked image of the constrained search may not be overwhelming.

INTRODUCTION

After acquisition and preprocessing (i.e., geometry processing and de-noising) of seismic data, stacking is the next step in the seismic data processing chain. Here, the concept of covering one subsurface element with many seismic waves (multi-coverage data) is exploited. This means, that redundant information belonging to the same subsurface element is searched and stacked coherently. The measure used within the stacking process for coherency evaluation of the data is usually semblance (Neidell and Taner, 1971). Since the traveltime of a seismic wave between a source and a receiver is not equal for varying source and receiver pairs, the coherency of a seismic event in the gather is described by the traveltimes of the corresponding seismic rays. In a second order approximation, the traveltimes of a seismic reflection can be described in a hyperbolic way (Hubral and Krey, 1980). This means, that a reflection event can be approximated by a hyperbola, which is characterized by the moveout. This forms the basis of the Normal Moveout (NMO) velocity analysis. The semblance value of a certain reflection event in a CMP gather is estimated by fitting a hyperbola to the data. For a single horizontal layer, the hyperbolic assumption is exact. In an arbitrary medium the hyperbolic assumption is approximate and applicable to small source receiver offsets. The fitted hyperbola is described by a single stacking parameter, the stacking velocity.

During the NMO velocity analysis for every CMP position and reflection event a hyperbola is fitted to the data such that the semblance value for this event is maximised. An extension of the CMP concept is the Common Reflection Surface (CRS) stack (e.g., Müller (1999); Mann (2002)), where the traveltime is no

longer approximated by a hyperbola, but by a hyperbolic surface since also neighbouring CMP positions are considered. Here three stacking parameters have to be searched instead of one. This means, that a hyperbolic surface is fitted to the data, NMO corrected, and stacked where the amplitude is attributed to the corresponding zero offset position of the data. This results in an enhancement of the stacking fold, and therefore, in a higher signal to noise ratio in the corresponding stacked section.

The CRS stacking procedure is implemented as a three dimensional semblance optimisation (e.g., Mann (2002); Müller (2007)). In the existing implementations the parameter estimation is split up in one-dimensional semblance optimisations for special geometrical configurations. This reduces the computational costs of the method. Due to the automated implementation, non-physical stacking parameters in areas of low coherency may occur, i.e., where no or weak reflection events are present. In these circumstances, the algorithm can determine geological unreasonable parameters. Therefore, we will introduce parameter search restrictions, that can be linked to geological features. These features may be known before the processing starts, which will then lead to a geological constrained parameter estimation.

In the following, we review the CRS theory, describe the current implementation, and introduce geological constrained parameter searches into the CRS implementation. Finally, we will show results of an initial test of these attempts on a marine industry data set from the Eastern Mediterranean / Levantine Basin.

THE CRS STACK

The conventional CRS formula is obtained by a Taylor series expansion of the traveltime at zero offset t_0 in midpoint and half offset coordinates, x_m, h, respectively. The traveltime expansion is according to , e.g., Jäger et al. (2001):

$$t^2(x_m,h) = (t_0 + \frac{2sin\beta_0}{v_0}x_m)^2 + \frac{2t_0 cos\beta_0}{v_0}(K_N x_m^2 + K_{NIP}h^2), \tag{1}$$

where v_0 is the near surface velocity, β_0 is the angle of emergence for the zero offset ray, K_N is the Normal-wave curvature, and K_{NIP} is the Normal-Incidence-Point (NIP)-wave curvature. The latter two parameters are linked to combinations of second order derivatives of the traveltime (Vanelle, 2002), but they can also be interpreted as wavefront curvatures measured at the acquisition surface for two artificial one way experiments. The Normal-wave is a wave front emerging from a circular exploding reflector element in depth centred at the NIP. The curvature of this wavefront in the acquisition surface is K_N. The NIP-wave is a wave front emerging from a point source at the NIP of the considered reflector and its curvature at the acquisition surface is K_{NIP} (for more details, see Hubral and Krey (1980)).

The CRS formula describes a hyperbolic surface (see Figure 1) which is parametrised in midpoint and half offset coordinates and can therefore be used as a stacking operator, that also considers the moveout towards neighbouring CMP locations (midpoints). This leads to some consequences for the resulting stacked section. First of all, since neighbouring CMPs are considered more traces compared to the CMP stack can be taken into account, i.e., the stacking fold is enhanced. This results in a better signal to noise (S/N) ratio in the final stacked section (Mann, 2002). As a result of the CRS stack we obtain the CRS attributes, which form the basis for many applications.

The stacking operator can not be arbitrarily enlarged, because we have approximated the traveltime by a second order Taylor series expansion. Therefore, we have to restrict the spatial extend of the CRS stacking operator. For the midpoint coordinate, the extend of the operator can be expressed in terms of the first projected Fresnel zone (Mann, 2002), which is linked to the lateral resolution of the seismic wave. The projected Fresnel zone around a receiver at the surface can be expressed as (e.g., Schleicher et al. (1997)):

$$\mid t_D(x) - t_R(x) \mid \leq \frac{T}{2}, \tag{2}$$

where t_D is the traveltime of a diffraction, t_R the traveltime of a reflection, and T the main period of the considered signal. The size of the projected Fresnel zone W_F can be approximated according to Mann (2002) by

$$W_F = v\sqrt{\frac{T^2}{4} + Tt_0} \approx v\sqrt{Tt_0}. \tag{3}$$

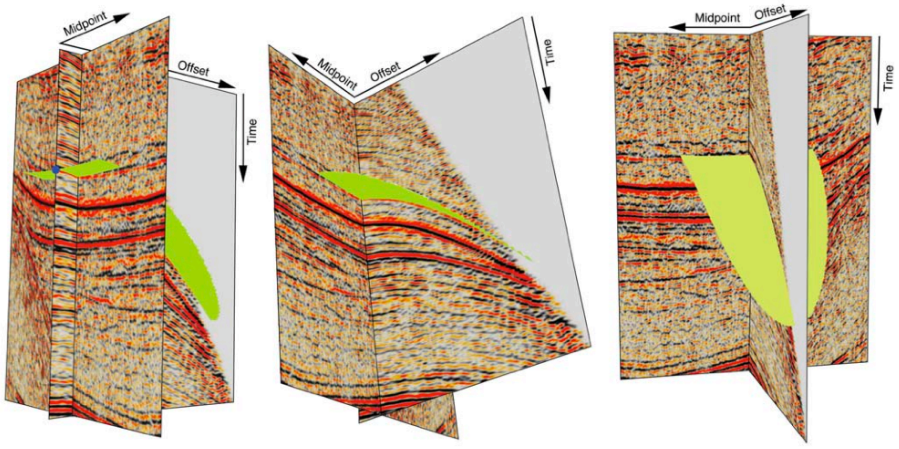

Figure 1: The hyperbolic CRS stacking operator in the midpoint and half data volume. All amplitudes on the green surface are stacked (Figure from Hertweck et al. (2007)).

In this equation a homogeneous half space is assumed and v corresponds to the average velocity in the overburden. For the half offset coordinate no explicit or approximate formula can be given. Here, we use the widely accepted rule of thumb that the target to offset ratio should not exceed 1. The spatial extend of the CRS stacking operator is crucial for the image quality. By a careful choice of the aperture the resolution of the CRS stack should never be worse than the resolution of the CMP stack.

IMPLEMENTATION

The following description mainly focusses on the CRS implementations of Mann (2002) and Müller (2007). We restrict the description to the 2D case, but it is straight forward to extend the approaches to the 3D case, see, e.g., Müller (2007). The implementation of the 2D CRS stack is realised as a three parameter optimisation procedure. By fitting a hyperbolic surface to the data, the semblance is optimised for every sample in the considered CMP gather. The semblance is defined after Neidell and Taner (1971) as:

$$S = \frac{\sum_{J=-W/2}^{W/2} \left(\sum_{i=1}^{N} f_{i,J+k(i)} \right)^2}{N \sum_{J=-W/2}^{W/2} \sum_{i=1}^{N} f_{i,J+k(i)}^2} \tag{4}$$

Here $f_{i,J}$ denotes the amplitude of the J^{Th} sample of the i^{Th} of N traces. A time window of width W is defined around the CRS operator at $k(i)$. A good choice for the length of the time window is the dominant period in the data. A drawback of the semblance criterion is the assumption of constant amplitude and phase along the stacking operator. In reality this is not always fulfilled since the reflection coefficient is angle dependent. Gelchinsky et al. (1985) present several alternative coherency criteria, which incorporate this fact correctly. Nevertheless, semblance is widely used, since the alternative coherency criteria are computationally more expensive.

The simultaneous optimisation of three parameters is a challenging task. Implementations simultaneously optimising all three parameters right from the start are currently under investigation. The method suggested by Santos et al. (2008) could be used as a good starting parameter set for a multidimensional optimisation. The current implementation simplifies the parameter search. The CRS operator is considered for typical acquisition geometries leading to 1-D optimisations. This speeds up the calculation, however, this procedure also reduces the number of traces involved in the parameter search which decreases the obtained semblance values. This approach is called the pragmatic search strategy (Mann, 2002). This search strategy and how to incorporate geological constrains is discussed in the next section.

CMP search

In the initial step the CMP configuration is considered, i.e., $x_m = 0$, and equation (15) reduces to a formula with two unknowns, the angle β_0 and the NIP-wave curvature:

$$t^2(x_m, h) = t_0^2 + \frac{2t_0 cos^2(\beta_0) K_{NIP}}{v_0} h^2. \tag{5}$$

This equation can be simplified via the equation

$$\frac{t_0 cos^2(\beta_0) K_{NIP}}{v_0} = \frac{2}{v_{NMO}^2} \tag{6}$$

to the conventional NMO formula

$$t^2(x_m, h) = t_0^2 + \frac{4h^2}{v_{NMO}^2}. \tag{7}$$

Thus, the first step of the pragmatic parameter search strategy reduces to automatic stacking velocity analysis. The stacking velocity is estimated by semblance optimisation for every sample in the data set. This is done by performing a grid search, with varying stacking velocity intervals. A stacking velocity interval is defined for the minimum time of the data as well as for the maximum time. For intermediate times the intervals are interpolated linearly. Then grid searches are performed in the interval with highest semblance to detect the best stacking velocity for every ZO sample. Since multiples or diffractions or other coherent noise may have high semblance values, the automatic determination of stacking velocities may lead to false results, if the velocity range does not exclude noise events above the semblance value of the reflection. This situation is illustrated in Figure 2.

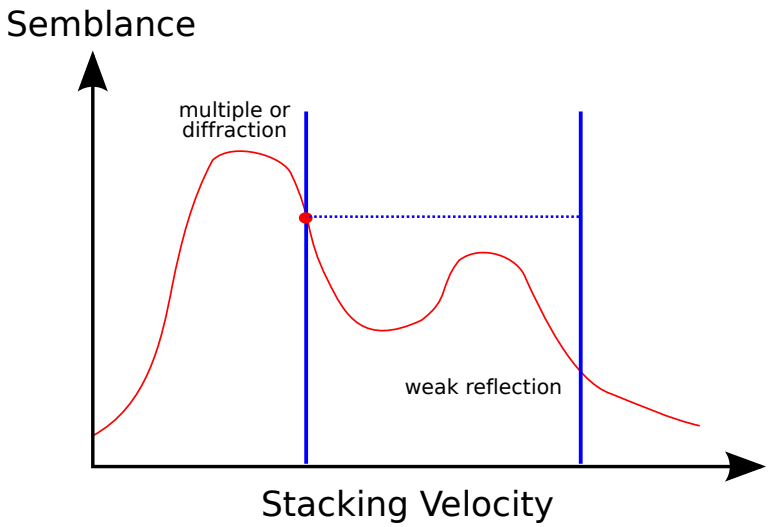

Figure 2: Erroneous automatic determination of stacking velocity. Coherent noise with large semblance may result in wrong stacking velocities. The boundaries of the stacking velocity range touch the noise event at higher semblance values than the reflections.

Obviously, to avoid this situation good a priori knowledge on the potential stacking velocities is essential. This could be done by incorporating only certain stacking velocity ranges as guides from previous processing steps. These guide velocities are usually picked manually during velocity analysis according to the expected geological situation. This step requires human intervention.

To restrict the parameter search without manual user interaction (i.e., velocity picking), we have to make assumptions on the geological situation and incorporate it into the automatic search. The RMS velocity of a layered medium is a slowly and smoothly varying function. Since the velocity often increases with depth we assume that the stacking velocity increases or stays constant with increasing time. Applied to the geological situation, this means that the sediments in the subsurface should not have strong negative velocity contrast such that the stacking velocity decreases. The assumption of a general increasing or constant stacking velocity can be applied to a wide range of geological situations. The smoothness of the stacking velocity is an additional option to check.

To incorporate this in an automated parameter determination, we implemented a dynamic stacking velocity range in the parameter search. We can restrict the lower boundary of the stacking velocity search interval to the determined stacking parameter of the previous sample. However, in the case of poor data quality (i.e., low S/N), this procedure is likely to generate non-physical results. Therefore, we only adjust the lower stacking velocity boundary for events with high semblance (see Figure 3 for an illustration of the scheme). Assuming increasing or constant stacking velocities we dynamically restrict the stacking velocity ranges in a data oriented way. This will provide a geologically more reasonable stacking velocity estimation. Guide functions or geological constraints also prevent the automatic algorithm from fluctuating parameter determination in the water column, to consider multiples, and large parameter fluctuations in deeper parts of the section. For low coherent events, e.g. for bad quality land data, the described procedure will not introduce restrictions to the search intervals.

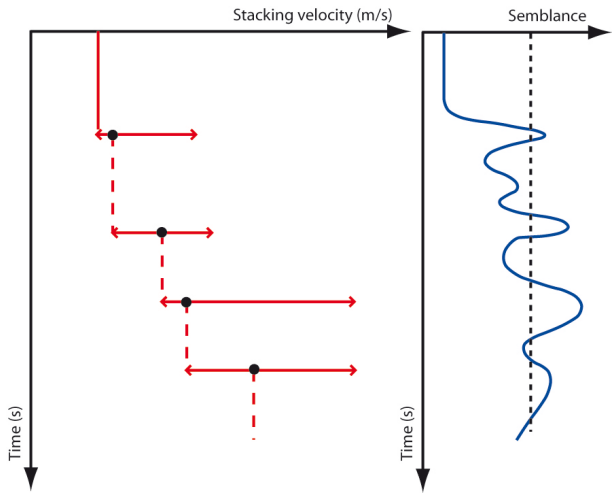

Figure 3: Schematic illustration of the dynamic stacking velocity range procedure. When an event reaches the coherency threshold (dotted black line), the lower boundary of the stacking velocity search interval is adjusted.

Zero offset search

The second parameter search is performed in zero offset sections, i.e., $h = 0$. The parameters are determined in the post-stack data domain, e.g., in the stacked section obtained from the first search. A drawback of the pragmatic search strategy is apparent if an automatically generated low quality CMP stacking result is generated. In this case the following ZO searches will not determine high quality parameters. To avoid this, one could generate a CMP stacking result manually by the conventional way. With processing experience, a sufficient image quality of the CMP stack can be achieved and the subsequent searches would benefit from this. Moreover, the determined stacking velocities can be used to guide the automatic parameter search.

Similar to the CMP search, the stacking parameters of the ZO search are determined by a grid search optimising the semblance. These searches are restricted to varying parameter intervals. In the zero offset

case, equation (1) reduces to

$$t^2(x_m, h=0) = (t_0 + \frac{2sin(\beta_0)}{v_0}x_m)^2 + \frac{2t_0 cos^2(\beta_0)K_N}{v_0}x_m^2. \quad (8)$$

In this equation two parameters are unknown. The assumption of plane waves, i.e., $K_N = 0$ (Hubral and Krey, 1980), leads to the equation:

$$t^2(x_m, h=0)_{K_N=0} = (t_0 + \frac{2sin(\beta_0)}{v_0}x_m)^2. \quad (9)$$

From this equation the angle of emergence can be determined by a one parameter optimisation. Afterwards the Normal-wave curvature K_N is determined by equation (8). Please note, that for the estimation of K_N the aperture of the optimisation has to be enlarged compared to the aperture for the determination of the angle of emergence. Otherwise, K_N would be determined close to zero, since this was assumed in equation (9) and already gave the optimal fit for the stacking operator. Finally, the remaining CRS parameter, i.e., the NIP-wave curvature, can be calculated with the help of the angle of emergence and the stacking velocity in equation (6). Although the pragmatic approach is computationally efficient, less traces are involved in the corresponding parameter searches leading to lower semblance values. Simultaneous searches provide higher quality and more smooth CRS parameter fields. All processing steps relying on CRS attributes would benefit from this.

Geological constrains to restrict the parameter searches are easily introduced into the zero offset optimisations. The search is performed in the stacked section, which already provides a first insight into the geological situation. Dominant structural information can be derived and incorporated into the parameter estimations. Since the angle of emergence is directly linked to the time dip of the considered reflection, the determination of the angle of emergence can be restricted to a certain interval. Without limits for the angle steep dipping noise events like diffractions might be detected particularly in areas of low S/N ratio. Such events may not correspond to the geological situation. In Figure 4 such a situation is displayed. In this data set from the North German Basin we hardly see geological structures in the section, but some coherent steep dipping events (from Baykulov et al. (2008)). From a priori geological knowledge we expect dominantly horizontal events for this area. If the interpreter has initial ideas on the expected dip we may limit the search range for the angle of emergence. Please note, that the determination of the curvature of the Normal wave also benefits from this procedure, since this parameter is determined from the same data, i.e., the stacked section. We assume that we approximately know the minimum and maximum time dip α_{min}, α_{max} of the main geological structures in the data. That means we can restrict the grid search intervals for the angle of emergence to $\alpha_{min} \leq \beta_0 \leq \alpha_{max}$. Alternatively, in the current implementation of the CRS stack a guide file can be introduced to the search, similar to the guide file in the CMP search. Restricting the grid search interval helps to force the estimation of the angle of emergence to the relevant area of interest. However, in the case of conflicting dips, where a strong unwanted event crosses a weak wanted event, the angle might be determined at the border of the corresponding search interval, i.e., it clips at the boundary of the search interval (see Figure 5). This clipping is an unwanted effect and is caused by a slow decrease of the coherency function of the strong unwanted event. By just restricting the search intervals the correct determination of the parameter for the weak but wanted event is nearly impossible.

To overcome these limitations, we have to pre-process the input data, i.e., the CMP section. If the geological situation allows, we modify the CMP stack in the desired way by restricting the dips in the sections and remove the unwanted events before the actual search is started. We apply dip filtering on the CMP stack sections for this purpose. Events that dip in the (t, x) domain are separated in the (ω, k) domain according to their dip (Yilmaz, 2001). A 2D Fourier transformation is applied transforming the (t, x) space into the (ω, k) space. In the (ω, k) domain, the data is decomposed into their time dips, and can therefore be discriminated. The data are filtered according to the desired dips., i.e. the unwanted dips are removed. This has to be done with a smooth taper function to avoid boundary effects in the (t, x) domain. Afterwards, the stack is transformed from the (ω, k) domain back into the (t, x) domain.

In the dip filtered stacked section we have attenuated unwanted events, e.g., diffractions or steep dipping coherent noise. With a proper choice of the filter parameters and the search interval, clipping effects at the borders of the search interval should not occur. Obviously this only works properly if the considered events

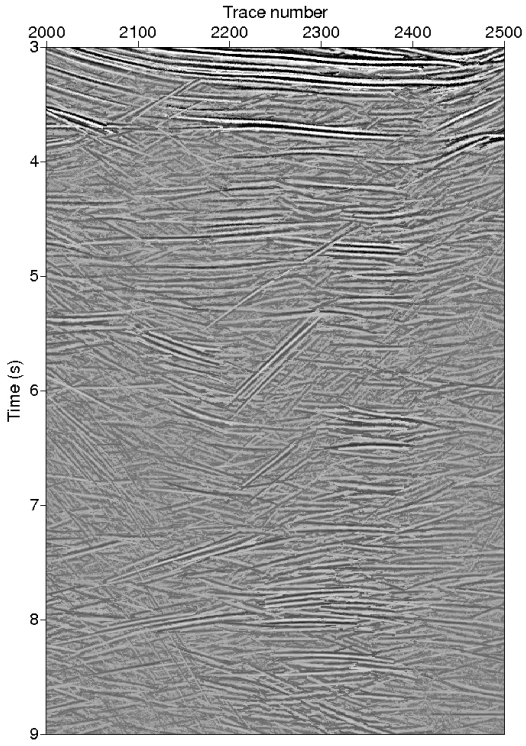

Figure 4: Stacked section from the North German Basin. Unwanted steep dipping coherent noise events occur in the section that hamper a geologically reasonable parameter determination.

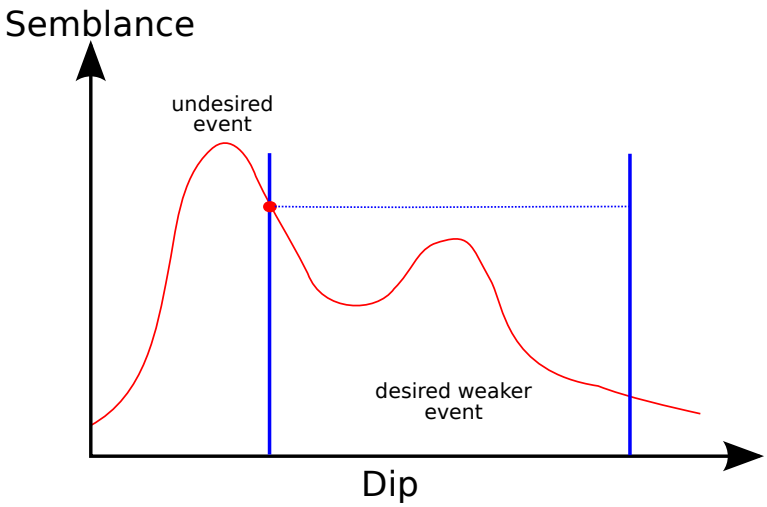

Figure 5: In a conflicting dip situation strong unwanted events may lead to wrongly determined dips at the border of the search interval.

have different dips than the unwanted noise or diffracted events. In many cases these circumstances are fulfilled. Alternatively, the procedure can be applied in certain data areas, e.g., as a windowed application. As mentioned above the determination of the normal wave curvature will also benefit from this procedure, since the CRS parameter estimation should be performed on reflection events. Please note that only the CRS attributes are determined in the dip filtered sections. The final ZO CRS stacked section is obtained from the original pre-stack data set using the improved CRS attributes.

CRS stack

After estimating the CRS attributes K_{NIP}, K_N and β_0, equation (1) is used for the CRS stack. Since this is done with the geological constrained parameters the stacking result will probably not reach maximum possible coherency values but will emphasize the geological relevant events. All following procedures using CRS stacking results like post-stack time migration will benefit from this procedure not just because of an improved stacked section but particularly because of improved CRS attributes.

Optimisation

According to the implementations of Mann (2002) and Müller (2007), the parameters determined by the pragmatic approach can be further optimised. The optimisation will in most cases not enhance the quality of the stacked section, but the determined parameters. This is of great importance to applications based on these CRS attributes. In Mann (2002) the CRS attributes are optimised jointly (simultaneous search) after their independent determination in the pragmatic approach. A flexible polyhedron search is used (Nelder and Mead, 1965). In contrast to that, Müller (2007) uses a technique based on simulated annealing (Kirkpatrick et al., 1983). Here, the flexible polyhedron search is extended by a so-called continuous optimisation by a simulated annealing algorithm (Press et al., 2002). This optimisation procedure can be applied after each initial grid search, i.e., after the CMP or the ZO search in the pragmatic approach, or for the final simultaneous optimisation of all parameters.

FIELD DATA EXAMPLE

To illustrate the application of geological constrains in the CRS parameter searches, we will process a subset of an industry data set from the Levantine basin in the Eastern Mediterranean Sea. The data covers the so-called Messinian evaporites, which result in strong vertical velocity contrast in the subsurface (bigger than $2000m/s$). The data was recorded using a $7175m$ streamer. Here, we use a maximum offsets of $3000m$. The CMP spacing is $12.5m$. In the following, we will discuss the CRS processing of the data and the results with special emphasis on the geological constrains introduced into the processing flow. For the sake of comparison we will also show processed sections using the conventional parameter searches without constraints.

First, we apply the stacking velocity constrains (Figure 6(c)) and compare the results of a fixed interval search (Figure 6(a)), a guide file constrained search (Figure 6(b)), and the reference result, picked manually from the stacked section (Figure 6(d)). As we can see, the result of the fixed interval search suffers from strong parameter fluctuations. These fluctuations are originating, e.g., from multiple reflections present in the data from about 3s onward. Although the search interval is set to higher values than typical multiple velocities, still stacking velocities at the boundaries of these search intervals are determined (see Figure 2 for illustration). The leads to the determination of lower stacking velocities than expected. Also some artefacts are present around 2.5s, which correspond to unreliably determined parameters (i.e., for low coherency events). When a guide file obtained from standard stacking velocity analysis is used with limits of ± 100m/s (Figure 6(b)), the automatically obtained stacking velocity field is significantly improved and less scatter occurs. The multiple reflections are not considered and artefacts are reduced. To obtain such a result without the knowledge of a guide file would be desirable. In Figure 6(c), we see the result of the dynamic geologically constrained search. We observe, that the scatter and the influence of the multiples are reduced. The overall impression is similar to the result obtained with the guide file but still more scatter is present. We also observe some slightly too high estimated velocities from 3s onward and some artefacts when comparing this result with Figure 6(b). However, the overall comparison of both search strategies

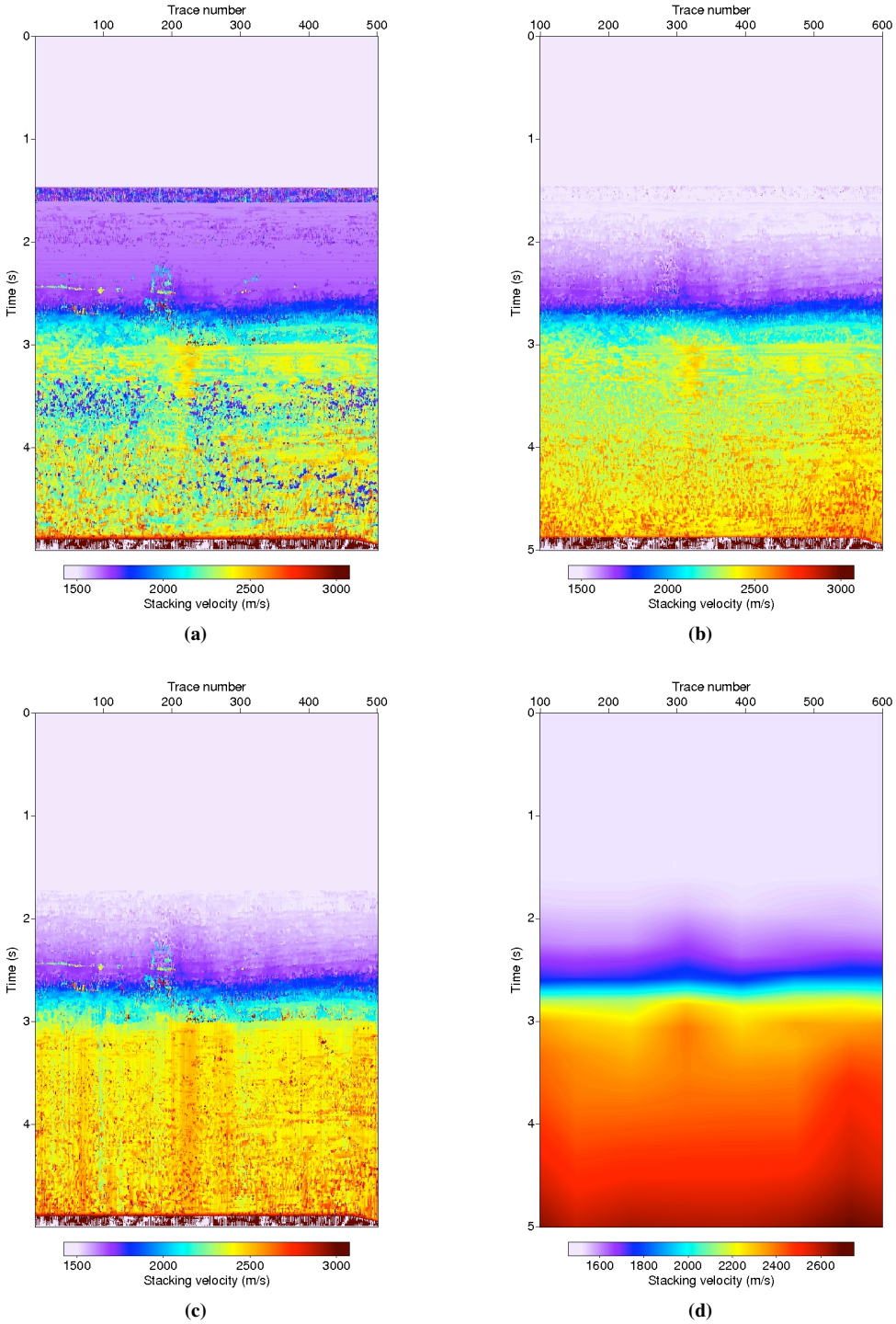

Figure 6: Stacking velocity fields from the CMP search. (a) fixed search interval result, (b) guide file constrained result, (c) dynamically geological constrained result, and (d) the reference result picked manually for the main events in the section (please note the different scale for image (d)).

is fairly well and we obtained comparable stacking velocity fields, generated fully automatically without using a guide file.

Continuing in the CRS processing chain, we perform the ZO searches, where we introduce geological constrains in the β_0 and R_N searches. For this purpose, we processed the data in the conventional way by restricting the parameter ranges and we also applied the geological constrained approach using dip filtering. First, we take a look at some of the stacking results. In Figure 7(a) the CMP stacking result is displayed. Many diffracting events are present which hamper the parameter estimation of the primaries. Fortunately, the diffractions have a significantly different time dip than the reflections and can therefore be removed by dip filtering. As a side effect of dip filtering noise generated by Radon filtering for multiple attenuation is also removed. The result after application of the dip filter can be seen in Figure 7(b). This section is almost free of unwanted events and will serve as input for the geological constrained ZO parameter estimation. In Figure 7(c) the removed events are displayed. Many unwanted events were removed.

We now take a look at the ZO parameter sections, i.e., the angle of emergence β_0 and the curvature of the Normal-wave K_N. In Figures 8(a) and 8(b), we see the results of the interval restricted search and the dip filtered search, respectively. As we can see from the comparison of both sections, the proposed search strategy shows less parameter fluctuations and focusses mainly on the reflections. In the result of the interval restricted search, we see some search interval clipping effects as illustrated in Figure 5 (angle values of ± 10 degree), especially in the areas of the steep dipping diffraction events. The search interval was already restricted to ± 10 degrees to focus on the reflections only. Via dip filtering, we could better force the parameter search to the relevant events in the section and thus determine the parameters in a less biased way.

Next, we will take a closer look at the K_N sections as determined by the second search in the ZO section. In Figure 8(c), we see the result of the interval restricted search and in Figure 8(d) the result of the dip filtered search. In comparison, we hardly see any differences beneath the ocean floor. In the area above the ocean floor, a top mute was applied in the interval restricted search, thus no parameters are determined here. However, when we take a closer look at the part of the section which was heavily contaminated with multiples (from 3s onward), it seems that the result of the dip filtering approach shows slightly less scatter. The difference between these two parameter sections appears to be small. One reason why the difference is small is the physical nature of the parameter itself. K_N is linked to the curvature of a reflector, which is for this section quite small since the interfaces are almost plane.

After the geological constrained parameter determination, the actual CRS stacking is the next step. For this stack the original pre-stack data are used. In Figure 9(a) the CRS stack is show where the automatic search for the stacking attributes were performed without constraints. Figure 9(b) shows the CRS stack where geological constraints were used in the search procedure. The stack with constrained search emphasise the geologically important events, i.e., the reflections. We observe less conflicting dip situations in Figure 9(b) and the noise level appears to be reduced particularly for times greater than 3s. Here the stack obtained from the constrained stacking attributes is more crisp. The constrained parameter search reduced the processing time and improved the image quality. Even if the improvement in the stack itself might not be too impressive, we have seen that the CRS attributes are generally better behaved and show less scatter. The improved CRS parameters are beneficial for subsequent procedures like, e.g., NIP-wave tomography. This might be even more important than a little improvement in the CRS stack itself. The smoother CRS attribute and their improved quality stabilises the tomography and reduces the computational time.

CONCLUSION

We have introduced geological constraints into the pragmatic parameter search strategy for the CRS attributes. If a priori information on the stacking velocities is available, this information can be incorporated into the search for the K_{NIP} attribute which is linked to the stacking velocity. One option for a constrained search is to use a guide file which specifies the range of the stacking velocities from previous velocity analysis. Even if no a priori information is available constraints on the stacking velocities may be applied. The stacking velocity function usually varies smoothly and for many geological situations increases with time. This may be used to constrain stacking velocities in an automated fashion. Stacking velocities and K_{NIP} usually show less scatter and are more smooth when constraints are used.

If a priori information of potential dips in the subsurface is available further constraints may be applied.

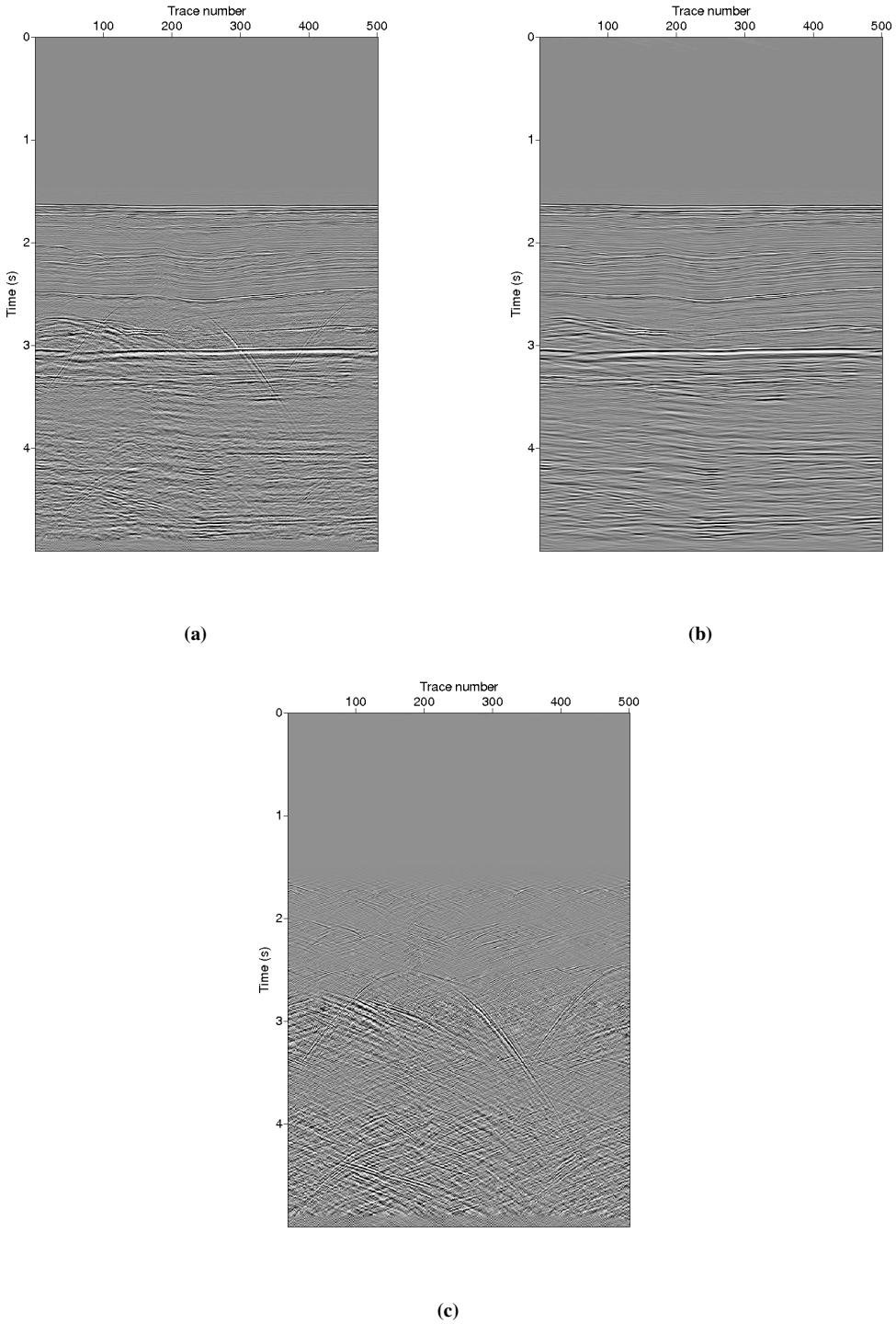

Figure 7: Results of the dip filtering before the ZO parameter searches.(a) Result for the CMP stack without preprocessing, (b) result after dip filtering, and (c) removed events.

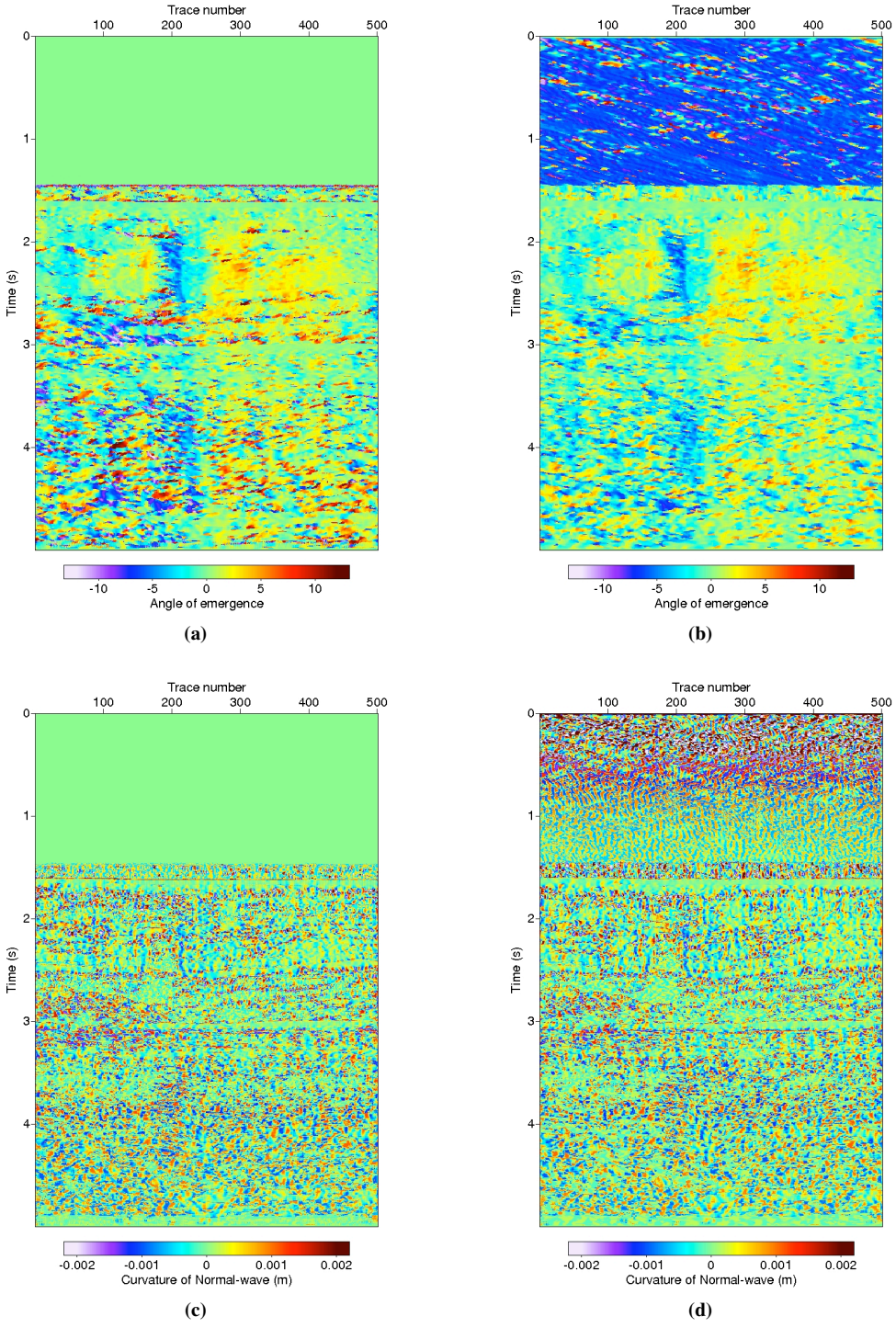

Figure 8: Results of the ZO parameter estimation. Angle of emergence determinations without (a) and with dip filtering (b), K_N estimations without (c) and with (d) dip filtering. The fluctuation above the ocean floor reflection in (b) and (d) are caused by weak coherent events in the water column (no top mute was applied).

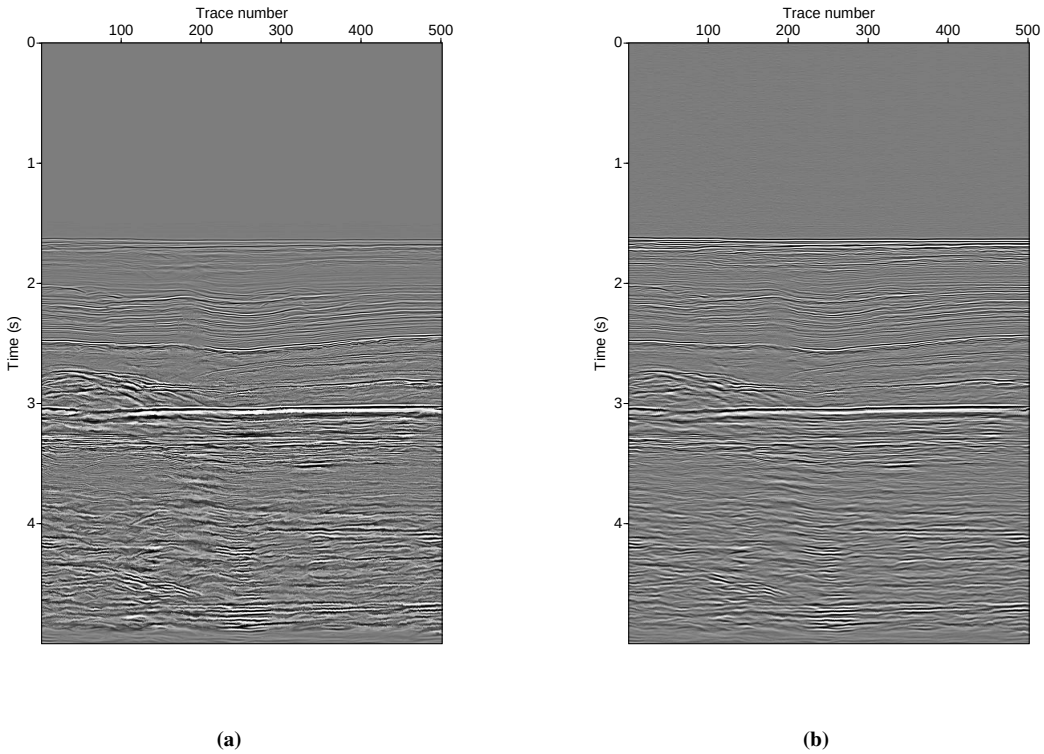

(a) **(b)**

Figure 9: (a) CRS stack without geologically constrained search. (b) CRS stack with geologically constrained search

This leads to dip filtering in the ZO section prior to CRS attribute determination of β_0 and R_N. This procedure steers the parameter search to reflections and avoids diffractions and other unwanted events. Again the result is a more smooth distribution of CRS attributes and reduced artefacts in the image.

CRS attributes obtained with constraints are particularly valuable for other processing steps based on these attribute (e.g., NIP-wave tomography, multiple suppression, pre-stack data enhancement, partial stacks). The difference in the CRS stacks obtained for CRS attributes with and without constraints may not be overwhelming. The positive influence on subsequent processing steps using these attributes, however, justifies the application of constraints. Moreover, since constraints usually limit the search ranges the CRS parameter determination is generally faster compared to a search without constraints. As soon as the constraints are specified, the search procedure itself is fully automatic as for the unconstrained search. The incorporation of constraints corresponds to dip and velocity filtering to obtain the stack. If the a priori information is wrong, desirable events might be missed.

ACKNOWLEDGEMENTS

We are grateful to the Applied Geophysics Group at the University of Hamburg, Germany, for fruitful discussions. This work was partially supported by the sponsors of the Wave Inversion Technology consortium, and the German Research Foundation (Hu698/14-1).

REFERENCES

Baykulov, M., Brink, H., Gajewski, D., and Yoon, M. (2008). Revisiting the structural setting of the Gl§ckstadt Graben salt stock family, North German Basin. *Tectonophysics*.

Gelchinsky, B., Landa, E., and Shtivelman, V. (1985). Algorithms of group and phase correlations. *Geophysics*, 4(50):596–608.

Hertweck, T., Schleicher, J., and Mann, J. (2007). Data stacking beyond CMP. *The leading Edge*, pages 818–827.

Hubral, P. and Krey, T. (1980). *Interval velocities from seismic reflection traveltime measurements*. Soc. Expl. Geophys.

Jäger, R., Mann, J., Höcht, G., and Hubral, P. (2001). Common-Reflection-Surface stack: Image and attributes. *Geophysics*, 66:97–109.

Kirkpatrick, S., Gelatt, C., and Vecchi, M. (1983). Optimisation by simulated annealing. *Science*, 220(4598):671–680.

Mann, J. (2002). *Extensions and Applications of the Common-Reflection-Surface Stack Method*. Ph. D. thesis, University of Karlsruhe.

Müller, N. (2007). *Determination of interval velocities by inversion of kinematic 3D wavefield attributes*. Ph. D. thesis, University of Karlsruhe.

Müller, T. (1999). *Die Methode des Common Reflection Surface stacks*. Logos Verlag, Berlin.

Neidell, N. and Taner, M. (1971). Semblance and other coherency measures for multichannel data. *Geophysics*, 71:482–497.

Nelder, J. and Mead, R. (1965). A simplex method for function minimization. *Computer Journal*, (7):308–313.

Press, W., Teukolsky, S., Vetterling, W., and Flannery, B. (2002). *Numerical Recipes in C++, Second Edition*. Cambridge University Press.

Santos, L., Schleicher, J., Costa, J., and Novais, A. (2008). Fast estimation of CRS parameters using local slopes. *WIT annual report*, pages 219–229.

Schleicher, J., Hubral, P., Tygel, M., and Jaya, M. (1997). Minimum apertures and fresnel zones in migration and demigration. *Geophysics*, 62:183–194.

Vanelle, C. (2002). *Traveltime based true amplitude migration*. P.h.D. thesis, University of Hamburg.

Yilmaz, O. (2001). *Seismic data analyses*. Society of Exploration Geophysicists, Tulsa.